

Directions for space-based low frequency radio astronomy

1. System considerations

J. P. Basart,¹ J. O. Burns,² B. K. Dennison,³ K. W. Weiler,⁴ N. E. Kassim,⁴
S. P. Castillo,⁵ and B. M. McCune⁶

Abstract. Although observations at the low end of the radio astronomy spectrum were the precursor of all work in radio astronomy, this portion of the spectrum has languished for decades while research at the upper radio frequencies has flourished. Previous work at low frequencies (below 30 MHz) has clearly shown that sensitive high-resolution ground-based observations are extremely difficult to make, if not impossible. Observation quality at low frequencies can leap forward using space-based interferometers. Radio telescopes such as these can be built principally from “off-the-shelf” components. A relatively low cost space program can make great strides in deploying arrays of antennas and receivers that would produce data contributing significantly to our understanding of galaxies and galactic nebulae. This paper discusses the various aspects of low-frequency telescopes such as past history and significant issues like sensitivity, interference, baseline calibration, wave scattering, and mapping. All aspects of the first stages of space-based, low-frequency radio telescopes can be accomplished with no dependencies on new types of hardware. The time has come to open the final electromagnetic frontier in astronomy.

Introduction

The purpose of this paper and paper 2 [Basart *et al.*, this issue] is to raise the awareness among astronomy practitioners and other people interested in astronomy of the need to stimulate interest in the area of low-frequency radio astronomy and of the technical problems involved in this field. The two papers give an overview of the major considerations required to do high-resolution low-frequency radio astronomy. For

our purposes here we define the low-frequency range to be from 0.3 to 30 MHz. Neither limit is exact, but they roughly delineate a frequency range in which high-resolution observations are extremely difficult, or impossible, to conduct from the ground. However, within this frequency range, many varied and exciting investigations can be conducted of the plasma universe.

Design studies were initiated by the authors for the purpose of laying the foundation for constructing and deploying a low-frequency aperture synthesis telescope in space. While these studies were not intended to be definitive or exhaustive, they did address the principal concerns of performing measurements in space and the hardware required to do so. However, many details of designing, deploying, and operating a space telescope were not addressed.

The science of radio astronomy was initiated near the lower end of the radio spectrum and subsequently migrated towards the higher end of the spectrum as microwave receivers and antennas evolved. Radio telescopes at high frequencies enjoy higher resolution than their low-frequency counterparts since resolution is proportional to λ/D where D is the diameter of the antenna (aperture) or array dimension, and λ is the wavelength. Shorter wavelengths also make it possible to build single apertures of high sensitivity and to build very high-resolution antenna arrays of a manageable

¹Department of Electrical Engineering, Iowa State University, Ames.

²Department of Astronomy, New Mexico State University, Las Cruces.

³Department of Physics, Virginia Polytechnic Institute, Blacksburg.

⁴Remote Sensing Division, Naval Research Laboratory, Washington, D.C.

⁵Department of Electrical Engineering, New Mexico State University, Las Cruces.

⁶Physical Sciences Laboratory, New Mexico State University, Las Cruces.

size on the Earth's surface. Additionally, microwave frequencies are sufficiently high to avoid severe disturbances from the ionosphere. The natural universe cooperated by minimizing interfering background emissions from the Galaxy at high radio frequencies and minimizing terrestrial tropospheric effects in the microwave region. Signal processing techniques have dramatically reduced atmospheric wave propagation disturbances even further and made it possible to extract more information from data than originally thought possible.

These natural and engineered effects caused astronomical activity to blossom at centimetric wavelengths, while withering at lower frequencies, especially at decametric wavelengths. As stated by the Radio Panel of the Astronomy and Astrophysics Survey Committee (Bahcall committee), "... the scientific potential of the long wavelength bands has barely been tapped, largely because of the difficulty in obtaining adequate resolution and the distortions introduced in the Earth's ionosphere" [Kellermann *et al.*, p. I-17, 1991]. Initial observations from space have been undertaken, but there have been no serious (i.e., funded) attempts to fully develop this portion of the electromagnetic spectrum since the two-spacecraft Radio Astronomy Explorer (RAE) series in the late 1960s and early 1970s. The Bahcall committee recognized the need to tap the scientific potential of low-frequency radio astronomy and "... recommends that an orderly program begin during the 1990's directed toward the development of low-frequency radio astronomy techniques on the ground and in space, ultimately leading to the establishment of a low-frequency, high-resolution radio astronomy telescope on the moon" [Kellermann *et al.*, p. I-2, 1991].

The principal ground-based activity in low-frequency radio astronomy occurred before aperture synthesis telescopes came into common use. A number of ground-based low-frequency instruments (see Table 1) were used to observe galactic and extragalactic emission. All of these instruments had very low resolution compared to current high-resolution arrays operating in the centimetric wavelength region, thus making it difficult to combine spectral information to extract detailed physics of the behavior of radio sources.

Need for Space-Based Telescopes

Below 100 MHz, ground-based high-fidelity, high-angular-resolution (i.e. arc-second) imaging of all but the simplest and brightest astronomical sources has been historically impossible due to the presence of the Earth's ionosphere. Time-variable gradients in total electron content (TEC) across the aperture corrupt visibility phase and reduce coherence times. A fundamental restriction is set by the scale size of turbulence in the Earth's ionosphere, which renders interferometric phase measurements essentially impossible for baselines longer than ~ 5 km unless procedures are employed to correct for the ionospheric effects. Thus the Clark Lake telescope with an aperture of ~ 3 km made excellent images over the frequency range from 16 to 123 MHz but at very modest angular resolution (typically $> 5-10'$). With this restriction in aperture the low-frequency limit for ground work is set by the ionospheric cutoff near $\sim 5-10$ MHz, with the ionosphere over Tasmania occasionally allowing observations down to 2 MHz [Cane, 1987] albeit with a resolution of only $\sim 10^\circ$. The $2'$ resolution Cambridge 38-MHz

Table 1. Telescopes Used for Low-Frequency Ground-Based Observations

Observatory	Frequency MHz	Best Resolution arc min	Reference
Cambridge	13.1	160	<i>Andrew</i> [1969]
Clark Lake	15-125	20-2.7	<i>Erickson and Fisher</i> [1974]
Fleurs	19.7	60	<i>Shain et al.</i> [1961]
Fleurs (reconstructed)	29.9	50	<i>Jones and Findlay</i> [1974]
Grakovo	10-25	18-7.4	<i>Braude et al.</i> [1978]
Llanherene	5-20	180-45	<i>Ellis</i> [1972], <i>Ellis</i> and <i>Hamilton</i> [1966]
Penticton	10, 22.2	115, 65	<i>Roger</i> [1969], <i>Caswell</i> [1976]

survey by *Rees* [1990a, b] is perhaps the highest resolution survey currently available within these aperture constraints.

The recent success of the new 74-MHz, 35-km VLA observing system has elegantly demonstrated that the powerful techniques of self-calibration and dual-frequency ionospheric phase referencing (DFIPR) can essentially remove this historical ionospheric restriction on aperture size [*Kassim et al.*, 1993]. Use of global positioning system (GPS) receivers at ground-based observatories offers the possibility of developing even more sophisticated ionospheric corrections techniques in the future. These are profound developments and may soon offer an opportunity to go to as high an angular resolution as desired from the ground in the poorly explored frequency range below 100 MHz. However, there are legitimate reasons to expect that these new ionospheric correction techniques will only be good to ~ 30 MHz, indicating that space-based observations will be required for high-angular-resolution work even at frequencies substantially above the nominal ionospheric cutoff near 5-10 MHz.

The most serious restriction to high-resolution ground-based work below 30 MHz is ionospheric amplitude scintillation. The phase variations scale precisely as the wavelength squared provided that no amplitude scintillation are present, and this precise scaling is used by DFIPR calibration of the low-frequency data. However, at frequencies below 30 MHz there is enough angular refraction in ionospheric irregularities that rays passing through different irregularities can cross, causing constructive and destructive interference. This causes the apparent amplitude of the signal to scintillate and its phase to wander in an almost random fashion, rendering even self-calibration difficult and making phase calibration virtually impossible. At most midlatitude sites amplitude scintillation will occur about 30% of the time at 30 MHz, making the data unusable for this fraction of the time. At lower frequencies the percentage will rapidly increase. Thus ~ 30 MHz appears to be a reasonable lower frequency limit for a future, sophisticated ground-based array.

In the modern era of radio astronomy there have been attempts from time-to-time to open the window on low-frequency radio astronomy from space. Radio Astronomy Explorers (RAE 1 and 2) of the 1960s and 1970s were the only totally dedicated radio astronomy missions to have flown, but they provided only tens of degrees of resolution and had low sensitivity. Radio astronomy receivers have been on approximately 25

other space missions [*Kaiser*, 1989], but these mainly used simple monopole antennas for solar system studies. Most of these missions concentrated on planetary and solar science, which have provided a rich source of interesting phenomena. An enormous discovery for Earth scientists by RAE 1, but a problem for radio astronomy because it increases the environmental noise, was the auroral kilometric radiation (AKR). RAE-2, orbiting the moon, presented evidence that there is extensive low-frequency emission from the Earth from communication and radar signals that is detrimental to low-noise radio astronomy observations. Both RAEs successfully studied Jupiter's low-frequency noise and measured low-frequency solar radio bursts.

In the RAE missions it became obvious that the Earth was a source of very strong radio emission at low frequencies. To reduce the system noise level due to terrestrially related emissions in the future, it will be necessary to place low-frequency telescopes in solar orbit well removed from the Earth, or behind the moon. Figure 1 [from *Kaiser*, 1990] shows the dramatic reduction in system noise when a lunar orbiting radio telescope goes behind the moon

Science

The Sun is the most intense astronomical source at low frequencies. Measurements below 2 MHz from space have provided information on morphology, brightness temperature, and physics of solar radio phenomena. The spacecraft ISEE 3 provided useful observations of electrons, plasma waves, and radio waves created by the initiation of type III bursts and the subsequent Langmuir waves that are produced. However, relatively few observations have been made of the Sun between 2 and 20 MHz [*Dulk*, 1990].

Unresolved bursts from Jupiter have been observed numerous times from the ground [*Carr and Wang*, 1990] and from space [*Desch* 1986]. The ionosphere limits ground-based observations to frequencies above about 7 MHz. The timing of the bursts is tied to Jupiter's rotation and occurs regularly for hectometric emission, but sporadically for decametric and kilometric emission. Long-term monitoring of the hectometric radiation may provide rotation period data of higher precision than present methods can provide [*Carr and Wang*, 1990].

Subsequent to the discovery of Jupiter bursts at low frequency, Saturn was found from Voyager observations to sporadically emit kilometric radiation (SKR) [*Desch*, 1986]. The emission occurred in the hun-

dreds-of-kilohertz region at power levels comparable to the Earth's AKR. The intensity variations in SKR are driven by variations in the solar wind. Curiously, Saturn's magnetic dipole field axis is not tilted with respect to its rotation axis [Ness *et al.*, 1981], yet the auroral emissions are strongly modulated by the planetary rotation.

Benefits of Low-Frequency Observations

Numerous astrophysical investigations can be pursued with low-frequency data. They principally involve plasma phenomena. For a review of the many possibilities see the book by Kassim and Weiler [1990]. We briefly summarize the benefits of low-frequency observations to the science of astronomy beyond the solar system.

Origin of cosmic rays. Perhaps the most fundamental question still remaining from the era of classical physics is the origin of cosmic rays. Cosmic rays represent the most energetic form of matter and trace the highest energy phenomena. At frequencies below 30 MHz there is a real possibility for probing the particle acceleration process in supernova remnants and addressing the origin of cosmic rays.

Galactic nonthermal background. In studies of the distributed nonthermal background emission of the Milky Way, different frequencies emphasize different physical processes. The surveys of γ ray emission are sensitive to the interaction of cosmic rays with the ambient interstellar gas; optical surveys emphasize stars and ionized hydrogen (HII) regions; and infrared surveys enhance visibility of the relatively cold interstellar dust. Radio frequency studies are most sensitive to the relativistic cosmic ray electrons and interstellar magnetic fields. However, there are problems in explaining the observed break in the cosmic ray electron energy spectrum near 3 GeV, which is equivalent to the background radio spectrum break at ~ 300 MHz. Low-frequency observations may be able to provide clues to the relevant loss and injection mechanisms.

Galactic diffuse free-free absorption. By observing a large number of extragalactic radio sources and determining their low-frequency spectra as a function of galactic latitude and longitude, it will be possible to measure the distribution of absorption by the diffuse interstellar gas in the Milky Way. Combining survey results at several frequencies available to a space-based interferometer with low-resolution higher-frequency maps from the literature, we can successfully separate the thermal absorption and nonthermal emission components of the Galaxy.

Interstellar scattering and refraction. It is generally accepted that small-scale ($\sim 10^9$ cm) fluctuations in electron density in the interstellar medium can diffractively scatter radio waves from a background source. Less clear is the ability of somewhat larger irregularities ($\sim 10^{13}$ cm) to refractively focus and defocus radio waves. The questions which can be addressed at low frequencies are What is the correct form of the irregularity power spectrum?, Is the irregularity spectrum ever anisotropic?, How common are refractive distortions and refractive scintillation?, and What is the origin of the turbulence and how is it distributed throughout the Galaxy?

Extragalactic sources. A low-frequency radio telescope array can detect thousands of discrete sources and study the brighter ones for such properties as integrated spectrum, surface brightness and spectral index distribution, and source counts versus intensity. This is especially important since owing to synchrotron radioactive lifetimes, the relativistic electrons which a space-based telescope detects are, in general, far older than those normally studied by radio astronomy.

Spectra. It has long been known that the radio spectral index (α) is a function of frequency and that the measurement of this frequency dependence is important for understanding the physics of the emission and absorption processes in the sources. At present, very little is known about source spectra at frequencies as low as 20 MHz, and practically nothing has been measured for frequencies less than 10 MHz.

Supernova remnants and pulsars. Low-frequency radio observations provide a unique means for investigating SNRs, their interaction with the interstellar medium (ISM), and the shock acceleration processes. A number of millisecond pulsars have spectra that are very steep with flux densities that continue to increase down to the lowest observed frequency of ~ 10 MHz. These pulsars, although nonpulsing owing to interstellar scattering at these frequencies, are among the strongest sources in the sky at 10 MHz.

Coherent emission. A very exciting possibility at low frequencies is the detection of coherent radiation. There are valid physical reasons to anticipate that the smaller distance between individual radiating electrons measured in terms of the electromagnetic wavelength is likely to amplify collective radiative modes.

Constraints on a Low-Frequency Array in Space

Once a low-frequency telescope is above the Earth's ionosphere, the biggest problem which limits the tele-

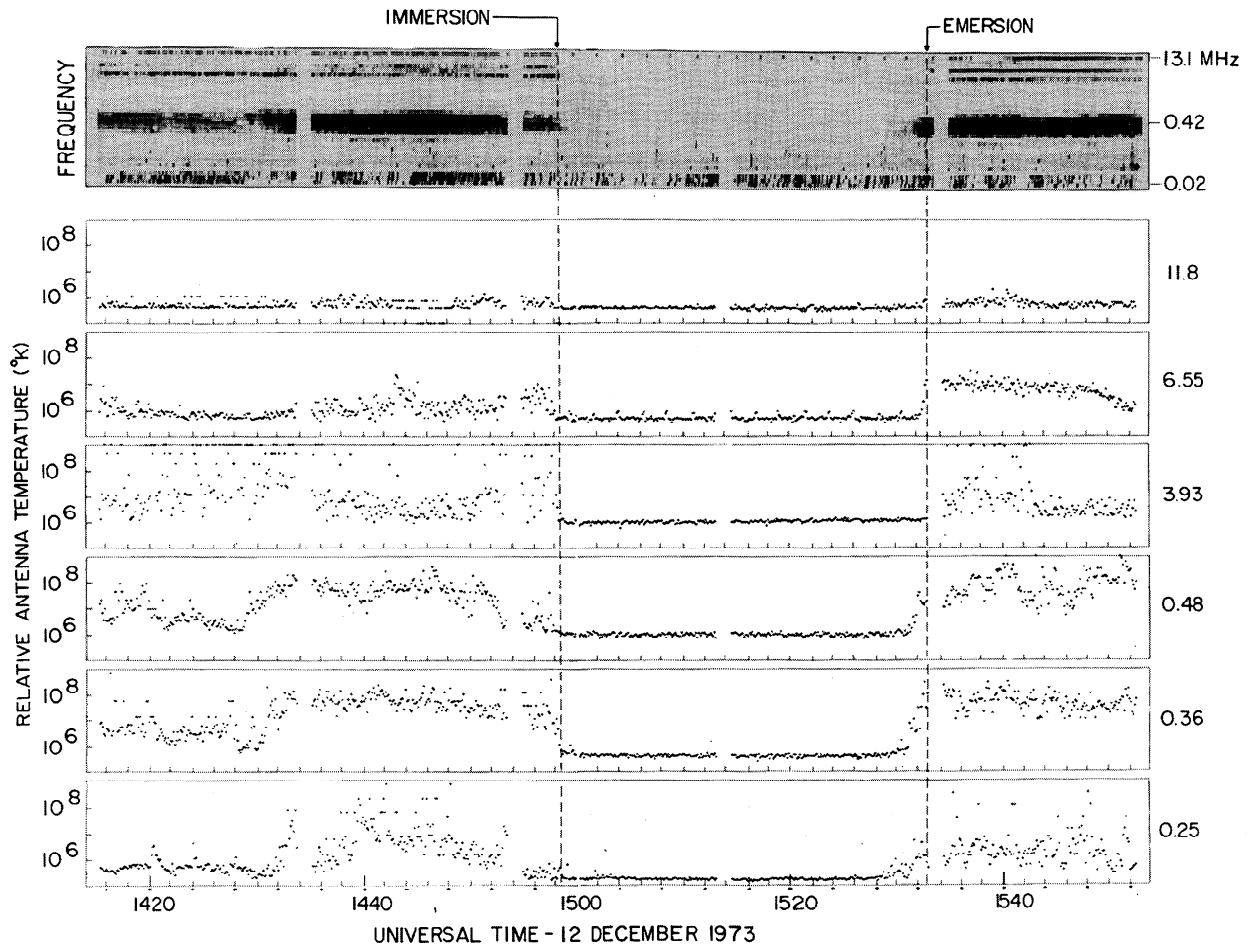


Figure 1. Evidence of interfering signals from Earth is shown by the decrease in intensity of received emission by RAE 2 when the spacecraft is behind the moon. Figure from Kaiser [1990]. Reprinted with permission of Springer-Verlag New York, Inc.

scope performance is interference as shown from RAE 2 data in Figure 1 [Kaiser, 1990]. At all frequencies shown, the intensity of emission from the Earth diminishes significantly when the satellite is far from the Earth or behind the moon. Sources of interference depicted in Figure 2 [Desch, 1990] are the AKR, lightning, communication signals, electrical machines (grouped under “spherics”), and the galactic background. The Sun and Jupiter are also sources of significant emission. Reviews of these various interference sources are given by [Erickson 1988, 1990] and [Desch, 1990]. A study of interference as seen by an orbiting radio telescope is given by McCoy, [1995] and McCoy *et al.* [1996]. In the frequency range of interest for low-frequency telescopes, approximately 0.3 to 30

MHz, the biggest interference problem to contend with is that of communication (including radar) signals.

Levels of Interference

In the frequency range of 0.1 to 1 MHz the dominant causes of interference are the AKR and type III solar bursts. AKR is generated on the Earth’s night-side at high terrestrial latitudes and could be caused by a maser plasma instability [Borovsky, 1988]. The daytime AKR interference is 40 to 50 dB below the nighttime level. Problems from AKR will be minimized by observing on the dayside below 0.8 MHz, while above 0.8 MHz there will be minimal AKR problems, both day and night, provided the receiver has strong filtering against frequencies below 0.8 MHz.

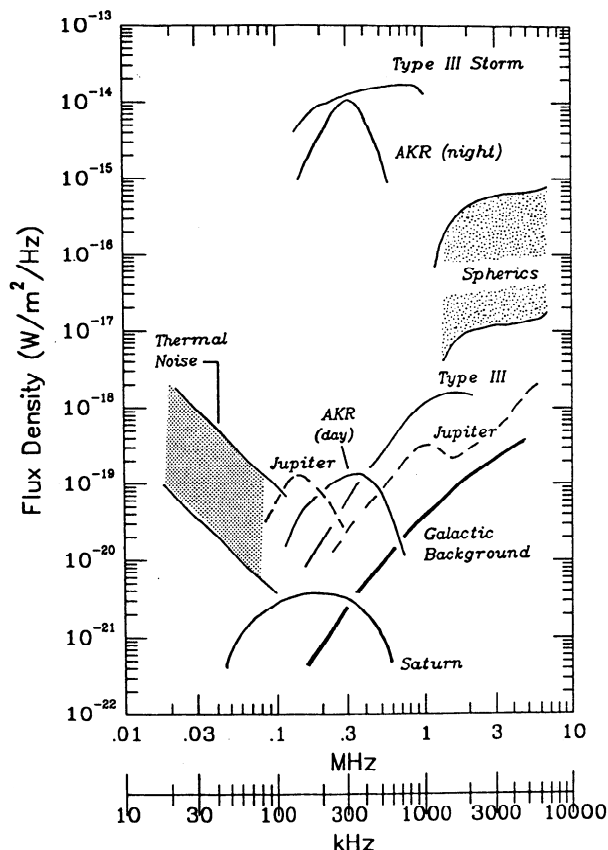


Figure 2. Strongest sources of noise in the Earth's environment below 10 MHz as observed from Earth except for the AKR which is referenced to a location at 25 R_E . Figure from Desch [1990]. Reprinted with permission of Springer-Verlag New York, Inc.

Type III solar bursts are generated by streams of high-energy electrons propagating outward from the Sun. The bursts have a wide continuum of emission at low frequencies and can best be avoided by observing during a minimum in the approximate 11-year solar cycle.

Moving up in frequency to the 1- to 10-MHz band, the strongest source of interference is caused by man-made radio emissions, but lightning can also be serious in this frequency range. Herman *et al.* [1973], using the RAE satellite, were the first to measure interference from the Earth at frequencies <10 MHz. The brightness temperature of the peak interference from Earth's nightside was 9×10^9 K (antenna solid angle was ≈ 1 sr for frequency ranging from 3.93 to 9.18 MHz for a double-sideband receiver with a 0-Hz IF and a 10- to 30-kHz IF bandwidth). This interference level is

stronger than the galactic background emission of $\approx 4 \times 10^4$ K at 9 MHz.

LaBelle *et al.* [1989] using the Active Magnetosphere Particle Tracer Explorers' Ion Release Module (AMPTE-IRM) satellite, located at 15 R_E , measured terrestrial background emission with an equivalent flux density of 6×10^{-17} W m $^{-2}$ Hz $^{-1}$ at the distance of the moon at 5 MHz. Of the artificially generated noise interference sources, communication signals are dominant. Other causes are swept-frequency radars, over-the-horizon radar (OTH), and ignition discharges. LaBelle *et al.* [1989] suggest that the terrestrial background emission may have risen by 20 dB in the 15-year span between the RAE and the AMPTE-IRM measurements with one possible cause being OTH (owing to the bursty nature of the emission and the equivalent transmitter power of a 500-kW transmitter). The interference generators are located below the ionosphere and frequently below the local plasma frequency, but their signals can leak through the ionosphere via erratic propagation paths. Since communication signals are generated around the globe (there is a longitudinal dependence due to some countries generating more signals than others), minimizing the reception of these signals by a radio telescope is quite difficult.

At the highest end of the suggested band for low-frequency telescopes, 10-30 MHz, Earth-based communication signals continue to be the dominating source of interference. An especially severe problem will be OTH-B (backscatter) radar. These radars transmit high powers between 5 and 28 MHz in order to create a detectable signal which is reflected from a target 2000-3000 km away from the radar. Even with significant attenuation from the ionosphere, the amplitude of a radar signal that leaks through the ionosphere can saturate a radio telescope receiver.

Jupiter and Saturn generate significant emission but usually intermittently. Jupiter's emission is stronger than Saturn's and covers the entire frequency range of interest to low-frequency telescopes in space. Saturn's emissions are principally confined to 1 MHz and lower. Two other outer planets, Uranus and Neptune, generate emission below 2 MHz, but it is sufficiently weak that we can ignore them as sources of interference.

Two frequency bands between 10 and 30 MHz are protected for radio astronomy by international agreement [Gergely, 1990]: 13.36–13.41 MHz and 25.55–25.67 MHz. Considerable interference still occurs in these bands, but this is dropping rapidly since no assignments have been made in these bands for more

than 10 years. The protected bands are the appropriate locations for future low-frequency radio telescopes not located on the lunar farside.

Sensitivity

Sensitivity is a critical issue in calibration because of the everchanging physical baselines of orbiting interferometers. Baseline changes set the time scale for integration of the signal which in turn affects the sensitivity. In source studies sensitivity is also critical over longer integration times because it determines the limit of brightness sensitivity that can be mapped for well resolved sources. The sensitivity of a single interferometer is

$$S_{\text{rms}} = \frac{\sqrt{2}kT_s}{\eta_a A \sqrt{\tau \Delta\nu}} = \frac{4\sqrt{2}\pi kT_s}{\eta_a D \lambda^2 \sqrt{\tau \Delta\nu}} \quad (1)$$

where k is Boltzmann's constant equal to 1.3805×10^{-23} J/K, T_s is the system temperature in K, η is the aperture efficiency, A is the aperture area in meters, τ is the integration time in seconds, $\Delta\nu$ is the bandwidth in hertz, λ is the wavelength in meters, and D is the directivity. If we take D in units of 200 and τ in units of megaseconds and assume 50 kHz for $\Delta\nu$, 50% for η_a , and 3×10^4 K for the system temperature at 30 MHz, we can rewrite (1) as

$$S_{\text{rms}} = 0.33 \left(\frac{D}{200} \right)^{-1} \left(\frac{\tau}{10^6} \right)^{-1/2} \times 10^{-26} \text{ W m}^{-2} \text{ Hz}^{-1} \quad (2)$$

For a directivity of 23 dB at 30 MHz and an integration time ranging from 100 s to 2 Ms, S_{rms} ranges from 44×10^{-26} to $0.033 \times 10^{-26} \text{ W m}^{-2} \text{ Hz}^{-1}$, respectively. The directivity is limited by the size of an antenna one could reasonably place on satellite, and the bandwidth of 50 kHz is a compromise chosen between a larger number to increase sensitivity and a lower number to reduce interference.

While it is useful to consider the sensitivity limit of the instrument caused by the system temperature noted above, the limiting sensitivity in a synthesized map is controlled by "confusion." Confusion can be defined as the contribution to the system temperature from all the unmodeled sources within the field of view (FOV) plus the contributions from all the sources that enter the sidelobes. Confusion noise will dominate at the lower frequencies because of the thousands of relatively bright sources that will be present within the large

primary antenna beam. However, it is difficult to quantify confusion because so little information is known about the source distributions at the frequencies and resolutions under consideration here. To illustrate the problem, consider an extrapolation of the 75-MHz situation. *Perley and Erickson* [1994] estimated that the confusion intensity at 75 MHz is $9.8 \times 10^{-26} \text{ W m}^{-2} \text{ Hz}^{-1} \text{ deg}^{-2}$. If we use a spectral index of $\alpha = -0.75$ (intensity $\propto \nu^\alpha$), the confusion intensity becomes $31.2 \times 10^{-26} \text{ W m}^{-2} \text{ Hz}^{-1} \text{ deg}^{-2}$ at 16 MHz. If we assume a primary beam size of 35° , the amount of flux density received is $\sim 4 \times 10^{-22} \text{ W m}^{-2} \text{ Hz}^{-1}$. It is quite important to minimize the size of the primary beam and to maximize the data coverage collected in the spatial frequency domain. These two topics are discussed in paper 2.

An important point to note here is that a significant percentage (perhaps $> 50\%$) of the flux in the primary beam will likely arise from a relatively small number of sources. For example, considering the 75 MHz Very Large Array (VLA) system with a 1° FOV, *Perley and Erickson* [1994] have shown that 50% of the flux from the ~ 200 sources in the field lies in only two sources. Hence, with a sufficient amount of data, it should be possible to properly deconvolve an image starting with models containing several sources.

For a space array the confusion problem is not well-defined because the source distributions required for the random walk analysis are essentially unknown at frequencies below 10 MHz at the resolutions being considered here. A reasonable approach to a practical solution is to map a given field at the high end of our frequency range (~ 38 MHz), where we can actually model the few brightest sources reasonably well from existing higher-frequency surveys (e.g., the 178-MHz 4C survey). After images are refined at the higher operating frequencies they can be propagated to the lower frequencies to be used as initial estimates for obtaining convergence of the deconvolution algorithms.

Interference Constraints on Imaging

There are several factors, in terms of interference, that potentially make interferometric observations superior to those of broad beam dipole antennas, as noted by *Thompson et al.* [1986]. These include finite bandwidth or delay beam effects and fringe-frequency averaging. In our analysis we first consider finite bandwidth effects. This will ultimately limit the useful field of view of the synthesized image. While most man-made interference is relatively narrow in bandwidth,

several interfering sources can occur simultaneously within the bandwidth of the telescope at these low frequencies. A wideband analysis of the noise is reasonable to undertake since it can indicate the most optimistic results of noise reduction via the bandwidth effect.

Following *Thompson et al.* [1986, p. 174], the distance away from the mapping field center at which the source intensity drops by a factor of R_b , owing to the bandwidth and a Gaussian-shaped band pass, is

$$r = 106\theta_b \frac{\nu_o}{\Delta\nu} \left(\frac{1}{R_b^2} - 1 \right)^{1/2} \quad (3)$$

where θ_b is the FWHM (full width at half maximum) of the synthesized beam (say 2"), $\Delta\nu$ is the bandwidth (50 kHz), and ν_o is the center frequency (25 MHz). For $R_b=0.1$, the diameter of the map field of view will be about 3°. Using the equation again to estimate how far away the image of the Earth must be from the field center to reduce the interference to a tolerable level ($R_b \approx 10^{-8}$) we find r to be impossibly large. Hence wide bandwidth alone cannot be used to escape broadband terrestrial interference, and narrowband interference will not be suppressed by this technique.

Fringe-frequency averaging can potentially be more effective than bandwidth effects in suppressing interference. Again, following *Thompson et al.* [1986, p. 476], the flux density of the interfering source which will be tolerable (10% of the system noise or less) is given by

$$S < 0.4\pi k T_s \left(\frac{\nu}{c} \right)^2 (2\Delta\nu)^{1/2} \left(\frac{dW}{dt} \right)^{1/2} \quad (4)$$

where T_s is the system temperature (3×10^4 K at 30 MHz) and dW/dt is the average fringe frequency rate (about 20 Hz). Thus the strongest source of interference that is tolerable is about $20,000 \times 10^{-26} \text{ W}^{-1} \text{ m}^{-2} \text{ Hz}^{-1}$. This is much below the peak interference from the Earth.

Thus it is clear that terrestrial interference will always be a problem unless (1) the array is far from the Earth in solar orbit, (2) the array is on the far side of the moon, or (3) sophisticated bandwidth selection techniques are used to avoid interfering signals.

Baseline Calibration

Baseline calibration is a serious problem for an interferometer with low-gain antennas at low frequen-

cies. The difficulty is based on the need for instantaneous calibration. For example, for a lunar orbiting telescope, perturbations by lunar mascons (mass concentration) to vary unpredictably by more than a wavelength. For an orbit 100 km above the Moon, the magnitude of the accelerations due to mascons is about 0.2 cm s^{-2} [*Sagitov et al.*, 1986]. The best currently available global models have residuals of about $\delta g = 7 \times 10^{-3} \text{ cm s}^{-2}$. Therefore the anomalous displacement over time interval, t , is just $(1/2)(\delta g)t^2$. The time period over which the baseline length deviates by $\lambda/2$ is then approximately

$$(\sqrt{2}\lambda / \delta g)^{1/2} \approx 50 \text{ s} \quad (5)$$

This is roughly the maximum coherent integration time using currently available models.

Data must be gathered on each calibration source in less than 50 s for baseline determination. The low sensitivity of each telescope (due to a wide beamwidth and high galactic background emission) and the weakness of the possible calibration sources cause this task to be very difficult.

Few good calibrator sources exist at 26 MHz. There are a number of extragalactic sources which are nearly unresolved in very long baseline interferometry (VLBI) observations, and therefore have sufficient compactness to be used as calibrators on baselines of at least 200 km. The correlated flux densities are generally less than $100 \times 10^{-26} \text{ W m}^{-2} \text{ Hz}^{-1}$ which, unfortunately, will render them useless during a 50 s integration. Within our galaxy the best calibrator sources are the Crab Nebula pulsar, and Jupiter when it is emitting bursts. The Crab pulsar is quite satisfactory with a flux density of $800 \times 10^{-26} \text{ W m}^{-2} \text{ Hz}^{-1}$ since the pulses are smeared into a continuum by the interstellar dispersion. Jupiter bursts are very strong (see Figure 2), but their sporadic nature diminishes their usefulness. Thus the calibrator situation below 30 MHz is difficult.

One possible alternative to calibrating the baseline at 26 MHz is to calibrate at a higher frequency, say 150 MHz. We gain in two ways with this increase: (1) the antenna directivity increases for the same physical antenna, and (2) the galactic background emission decreases. A disadvantage is that the fluxes from the sources are decreasing with increasing frequency. The improvement goes as $\nu^{(1.5+\alpha)}$ where the directivity improves as ν^2 , the galactic background decreases approximately as $\nu^{0.5}$, and α is the spectral index of the source ($S \sim \nu^\alpha$). There is an overall benefit at a higher frequency since the spectral indices for nonthermal

calibration sources lie roughly in the range from -0.2 to -1.0 . For a system temperature (sky dominated) of 400 K at 150 MHz, an aperture efficiency of 0.5, a bandwidth of 50 kHz, an integration time of 50 s, and a directivity of 10^3 , the rms flux density is approximately $3 \times 10^{-26} \text{ W m}^{-2} \text{ Hz}^{-1}$. With this sensitivity there are dozens of radio sources detectable; however, their potential as calibrators is limited because many will be resolved for the long baselines in this system. Nevertheless, it may be possible to calibrate the baselines at 150 MHz.

The highest accuracy in baseline calibration is derived from the fringe frequency, f , relationship to baseline, B , changes. That is,

$$f = \frac{1}{\lambda} \hat{s} \cdot \frac{dB}{dt} \quad (6)$$

where s is a unit vector in the source direction, and t is time. Using the error expression for frequency from Thompson *et al.* [1986, equation 12.27], the error magnitude on dB/dt is $\approx 0.8 \text{ cm s}^{-1}$ for a 400-K system temperature, 1.2-K source temperature, 50-s integration time, and 50-kHz bandwidth. So in the 50-s integration time the accumulated uncertainty in B is $\approx 40 \text{ cm}$.

The calibration method would then involve tracking baseline changes over some indefinite period of time and using this information to calibrate the fringe phase at lower frequencies. The fringe phase would then lack absolute calibration, and therefore absolute positional information would be lost, but the changes in the fringe phase would carry structural information. The coherence would be broken when the continuity of the baseline tracking is lost.

At least two sources are needed for calibrating the baseline. We can create multiple beams with subarrays of spherical array (see paper 2) and observe the calibrators plus the program sources simultaneously and maintain the integration time. All three beams could be essentially identical using spherical arrays.

A possible method of completely circumventing the standard calibration approach using astronomical sources is to use the GPS. Methods are continuously being refined to improve the accuracy of position determinations, especially differential positions between two sites. This becomes an interesting alternative approach to baseline calibration at low frequencies because of the lower accuracy required in determining the linear position (decreases proportionally to the increase in wavelength).

Interstellar and Interplanetary Scattering

Irregularities in the density of ionized gas in the interstellar and interplanetary media scatter radio waves, effectively broadening the image of a sufficiently compact source. Since the scattering angles scale approximately as λ^β where $\beta \approx 2$ [Rickett, 1977], we can expect this effect to be quite important at low frequencies. We do not have observations from space of the angular broadening of radio sources at low frequencies, so accurate formulation of scattering sizes is not possible (see discussion by Spangler and Armstrong [1990]). However, somewhat realistic approximations can be made, as shown by the authors in the above two references.

One source of scattering occurs in the interstellar medium. The turbulent scattering material in the Galaxy is highly inhomogeneous in distribution. There does, however, seem to be disk and halo components. High galactic latitude lines of sight are affected primarily by the halo component and typically suffer a moderate degree of scattering. The nominal high-latitude scattering magnitude scaled to 25 and 13 MHz implies scattering angles of 3 and 14 arc sec, respectively. Therefore fringe visibilities will be significantly suppressed on baselines of $> 800 \text{ km}$ and $> 330 \text{ km}$ at 25 and 13 MHz, respectively. There is considerable variation from one line of sight to another, such that these numbers could vary by a factor of at least 2 or 3. "Holes" in the interstellar medium due to the irregular distribution of electrons would possibly permit observations to a resolution of 1 arc sec along various lines of sight.

At low galactic latitudes the scattering is generally much larger, particularly towards the inner galaxy. Near the galactic plane scattering angles of the order of arc minutes at 25 MHz are to be expected. It is also noteworthy that scattering in the disk is highly variable from one line of sight to another. Scattering in the disk is evidently strongly affected by a distributed population of quite small structures which when intercepted produce heavy scattering.

For all situations at 25 MHz and below, interstellar scattering is strong, and, consequently, the resultant blurring is irrecoverable.

A second source of scattering is the interplanetary medium (IPM). As the IPM flows across the line of sight, the phase length fluctuates in time. The temporal spectrum of the phase fluctuations will have the same wave number dependence as the spatial spectrum, $P(q)$, of density fluctuations in the IPM, which is of the form [Lee and Jokipii, 1975]

$$P(q) = C_N^2 q^{-\alpha} \quad q_o < q < q_i \quad (7)$$

where q is the spatial wave number, and q_o and q_i are the outer and inner scales of the density fluctuations, respectively. The strength of turbulence, C_N^2 , is in general a function of distance from the Sun. An expression for C_N^2 , used by Spangler and Armstrong [1996] for estimating scattering sizes, is

$$C_N^2 = 3.9 \times 10^{15} (R/R_s)^{-4.05} \quad (8)$$

where R is the distance from the Sun, and R_s is the solar radius (7×10^{10}). The power law exponent, α , is probably quite close to the "Kolmogoroff" value of 11/3 for the IPM.

As the two elements of an interferometer are separated, their interplanetary phases become increasingly decorrelated. Consequently, the fringe phase of the interferometer shows random fluctuations, the magnitude of which increase with baseline length. These fluctuations reach approximately 1 rad in size on baselines of 80 to 300 km at 13 MHz and of 200 to 700 km at 25 MHz in the antisolar hemisphere. The uncertainty in the limiting baseline reflects possible solar-cycle variations as well as the range of elongations (90° to 180°). Certainly, high-resolution observations will have to be made in the antisolar hemisphere. In any case, there are serious limitations to the maximum usable baselines.

Considering the size of the isoplanatic patch, the phase fluctuations may be less severe than as discussed previously. The IPM scattering will increase the angular size of the radio source to the extent that it will exceed the size of the isoplanatic patch. Consequently, the observed phase is averaged over many independent lines of sight, which reduces the amplitude of the phase fluctuations. This in turn allows a longer coherent averaging time than what would otherwise be assumed.

Mapping Difficulties

Most of the techniques developed for microwave radio astronomy can be applied to low-frequency radio astronomy. Aperture synthesis and signal processing techniques are directly transferable. The principal differences between microwave and low-frequency telescopes and techniques are the form of the hardware, strong plasma effects on wave propagation, and extended mapping procedures. We will briefly discuss two considerations that are especially important to

space-based low-frequency radio astronomy; they are isoplanatism and noncoplanar arrays. These items have a strong impact on the process of mapping the data and require rigorous attention when a telescope and processing software are implemented. However, for our purposes here, we keep our remarks brief.

Isoplanatism

Simplistic processing of interferometric data assumes that within a "local" region of the electromagnetic wave propagating medium, waves from celestial sources are delayed by the same amount while traveling through this medium to reach the antennas in the interferometer. This is the property of isoplanatism. The "local" region for which a constant delay is assumed is called the isoplanatic patch. With an interferometer above the ionosphere we avoid the restrictions of the isoplanatic patch of that region as discussed by *Subrahmanya* [1991]. However, we are subject to the isoplanatic patch size of the IPM. The angular size of the isoplanatic patch in the IPM may be as small as 1 arc sec which is smaller than the synthesized beam. This condition means that special considerations must be taken while mapping. The most rigorous approach to mapping in such a situation is to divide the primary beam of each antenna into cells over which the delay in the IPM can be considered constant [Schwab 1984]. One then solves for phases in each cell. To reduce the computational burden of the rigorous method, another approach was suggested by *Subrahmanya* [1991], in which the propagating medium spanned by the telescope is subdivided into cells with constant phase delay within each cell. One then proceeds to solve for the phases within each cell. However, any particular processing approach used to overcome the small size of the isoplanatic patch can significantly increase the processing time. With the rapid increase in computer power each year, this problem should be manageable by the time low-frequency space arrays are in use.

Wide-Field Imaging

Telescopes in orbit using antennas with wide beam widths force us to address the problem of imaging with noncoplanar arrays (see *Perley* [1989] for a rigorous discussion of noncoplanar mapping). Except for snapshot observations, all arrays with non east-west spacings are noncoplanar and measure a three-dimensional (3 D) visibility function. Therefore a two-dimensional (2 D) Fourier transform of the measured visibility data

introduces phase errors that increase with distance from the phase center. At low frequencies where the field of view is large these errors can become severe. Solutions to this problem must be considered for a space based array.

The “3-D” problem. The visibility phase ϕ measured by an interferometer can be expressed as

$$\phi = 2\pi (ul + vm - w\theta^2 / 2) \quad (9)$$

where (u,v) are the standard baseline components in a plane normal to the source, and (l,m) are their conjugate direction cosines in the sky plane; θ is the distance from a map feature to the phase center (center of synthesized field of view), λ is the observing wavelength, and w is the third dimension in the visibility plane, perpendicular to the standard (u,v) plane, that becomes nonzero for the case of noncoplanarity. The “3-D” problem arises when the entire primary beam, which for a space array will cover a significant fraction of the sky, contains thousands of discrete sources which will need to be deconvolved from a synthesized map in order to achieve high sensitivities. In this case θ is driven by the field of view, that is, $\theta \propto \lambda$. Thus even though $w \propto 1/\lambda$, the phase error $\Delta\phi$ which results when the w term is ignored is $\propto w\theta^2 \propto \lambda$. Hence, for a fixed array size, phase errors tend to increase linearly with increasing wavelength and become quite significant at the lowest frequencies.

Practical Solutions. A solution to the 3-D imaging problem for low frequency VLA observations has been successfully implemented within the Software Development Environment (SDE) imaging package developed by T. Cornwell (see URL http://www.nrao.edu/dataprocessing/sde/this_dir.html). Cornwell's polyhedron algorithm DRAGON breaks up the 3-D “image volume” into many 2-D “facets,” each with its own “dirty beam.” After each facet is properly CLEANed with the appropriate point spread function, the 3-D image volume (with a spherical surface) is then projected back on to a 2-D image plane. The power of DRAGON is that it achieves comparable sensitivity to that obtained with a full 3-D transform but at a great computational savings. Currently, 327-MHz VLA data processed through DRAGON achieves thermal or classically confusion-limited sensitivities on a routine basis [Frail, et al. 1994, 1995]. Since there are typically hundreds of confusing sources in the primary beam, it is essential to have good (u,v) coverage for processing space-based low-frequency data in a manner that reduces confusion.

The key computational driver for extending the polyhedron algorithm to lower frequencies is the number of facets N that are required. Cornwell has shown that

$$N = \lambda B / D^2 \quad (10)$$

where B is the baseline length. Operating at 75 MHz at the VLA gives $N \sim 225$ for “A” array observations. For a space-based instrument with a 20° FOV providing an angular resolution of ~ 10 arc sec, $N \sim 10,000$, or approximately 50 times larger than largest currently tractable problems. DRAGON has recently been ported to a multiprocessor SGI Power Challenge array, where $N \sim 200$ -300 deconvolutions typically require at day or two of processing time. Significant improvements in speed are expected as parallelized coding techniques are advanced. Nonetheless, expansion of the polyhedron algorithm to a space array will require significantly higher computational power than is now commonly available, implying that additional thought should be given to narrowing the FOV further. However, with the present rate of increase in computer speed and the increasing sophistication of parallel processing techniques, solutions to the 3-D problem are computationally less formidable than once thought and certainly conceptually well in hand. At the rate computer power has been increasing, it is possible that sufficiently fast machines will be available by the time space arrays are operating early in the next century.

Summary and Conclusions

Very little high-resolution radio astronomy has been undertaken at frequencies below 30 MHz. The Bahcall committee has made it clear that a low-frequency program should be initiated in the 1990s. Many interesting science investigations can be undertaken, most of which relate to the plasma universe. Hardware for low-frequency space arrays is relatively undemanding, but there are several other problems to contend with when making high-resolution images. Wide primary beams and non-coplanar arrays require 3-D mapping (Fourier transform) that demands enormous amounts of computer processing time per image. Many “confusing” sources enter the antenna beam causing the need for deconvolving the sidelobes from the data. The accurate portrayal of the confusing sources requires collecting a large number of data points in the spatial frequency (u,v) domain. Also terrestrial interference has strong implications on the quality of mapping that can be accomplished, but this can be solved by placing in-

terferometers in solar orbit far from the Earth or on the far side of the moon. Near-Earth orbits may be possible locations for telescopes with careful monitoring and selection of observation frequencies. Interstellar and interplanetary scattering place limits on the resolution, but leave a window open around 20 to 30 MHz for which resolutions of approximately 2 arc sec could be obtained. Reasonably good results can be obtained to 10 MHz and perhaps somewhat lower. This resolution is very compatible with that of the VLA, and maps in the low-frequency region of the radio spectrum would add significant spectral knowledge about many radio sources and interstellar phenomena.

Acknowledgments. We thank the reviewers for very helpful suggestions. This work was partially supported by NASA Grant NAG9-396.

References

- Andrew, B. H., A survey of the anticentre region of the Galaxy at a frequency of 13.1 MHz, *Mon. Not. R. Astron. Soc.*, **143**, 17-25, 1969.
- Basart, J. P., J. O. Burns, B. K. Dennison, K. W. Weiler, N. E. Kassim, S. P. Castillo, and B. M. McCune, Directions for space-based low frequency radio astronomy, **2**, *Telescopes*, *Radio Sci.*, this issue.
- Borovsky, J. E., Production of auroral kilometric radiation by gyrophase-bunched double layer-emitted electrons: Antennae in the magnetospheric-current regions, *J. Geophys. Res.*, **93**, 5727-5740, 1988.
- Braude, S. Y., A. V. Megn, B. P., Ryabov, J. K. Sharykin, and I. N. Zhouck, Decametric survey of discrete sources in the northern sky, *Astrophys. Space Sci.*, **54**, 3-36, 1978.
- Cane, H. V., Tasmanian low frequency galactic background surveys, in *Radio Astronomy from Space*, Workshop 18, edited by K. W. Weiler, pp. 289-292, Nat. Radio Astron. Obs., Green Bank, W. Va., 1987.
- Carr, T. D., and L. Wang, Monitoring Jupiter's hectometric emission, in *Low Frequency Astrophysics from Space*, edited by N. E. Kassim and K. W. Weiler, pp. 113-117, Springer-Verlag, New York, 1990.
- Caswell, J., A map of the northern sky at 10 MHz, *Mon. Not. R. Astron. Soc.*, **176**, 601-616, 1976.
- Dennison, B., et al., The low frequency space array, in *Radio Astronomy from Space*, Workshop 18, edited by K. W. Weiler, pp. 305-313 Nat. Radio Astron. Obs., Green Bank, W. Va., 1987.
- Desch, M. D., Solar System Radio Astronomy at Low Frequencies, in *Radio Astronomy from Space*, Workshop 18, edited by K. W. Weiler, pp. 239-253, Nat. Radio Astron. Obs. Green Bank, W. Va., 1986.
- Desch, M. D., A quantitative assessment of RFI in the near-earth environment, in *Low Frequency Astrophysics from Space*, edited by N. E. Kassim and K. W. Weiler, pp. 70-78, Springer-Verlag, New York, 1990.
- Dulk, G. A., Solar Radio Astronomy at Low Frequencies, in *Low Frequency Astrophysics from Space*, edited by N. E. Kassim and K. W. Weiler, pp. 85-96, Springer-Verlag, New York, 1990.
- Ellis, G. R. A., Radio observations of the Gum Nebula below 20 MHz, *Proc. Astron. Soc. Aust.*, **2**, 158-159, 1972.
- Ellis, G. R. A. and P. A. Hamilton, Cosmic radio noise survey at 4.7 Mc/s, *Astrophys. J.*, **143**, 227-235, 1966.
- Erickson, W. C., Radio interference in the near-earth environment, *JPL Publ. 88-30*, Jet Propul. Lab., Pasadena, Calif., 1988.
- Erickson, W. C., Radio noise near the earth in the 1-30 MHz range, in *Low Frequency Astrophysics from Space*, edited by N. E. Kassim and K. W. Weiler, pp. 59-69, Springer-Verlag, New York, 1990.
- Erickson, W. C., and J. R. Fisher, A new wideband, fully steerable decametric array at Clark Lake, *Radio Sci.*, **9**, 387-401, 1974.
- Frail, D. A., N. E. Kassim, and K. W. Weiler, Radio imaging of two supernova remnants containing pulsars, *Astron. J.*, **107**, 1120-1127, 1994.
- Frail, D. A., N. E. Kassim, T. J. Cornwell, and W. M. Goss, Does the Crab have a shell?, *Astrophys. J.*, **454**, L129-L132, 1995.
- Gergely, T. E., Status of low frequency radio astronomical allocations at the 1992 World Administrative Radio Conference (WARC-92), in *Low Frequency Astrophysics from Space*, edited by N. E. Kassim and K. W. Weiler, pp. 79-81, Springer-Verlag, New York, 1990.
- Herman, J., J. Caruso, and R. Stone, Radio Astronomy Explorer (RAE), I, Observations of terrestrial radio noise, *Planet. Space Sci.*, **21**, 443-461, 1973.
- Jones, B. B. and E. A. Findlay, An aperture synthesis survey of the galactic plane, *Aust. J. Phys.*, **27**, 687-711, 1974.
- Kaiser, M. L., Observations of non-thermal radiation from planets, in *Plasma Waves and Instabilities at Comets and in Magnetospheres*, Geophys. Monogr. Ser. vol. 53, edited by B. T. Tsurutani and H. Oya, pp. 221-237, AGU, Washington, D. C., 1989.
- Kaiser, M. L., Reflections on the radio astronomy explorer program of the 1960s and 70s, in *Low Frequency Astrophysics from Space*, edited by N. E. Kassim and K. W. Weiler, pp. 3-7, Springer-Verlag, New York, 1990.
- Kassim, N. E., R. A. Perley, W. C., Erickson, and K. S. Dwarakanath, Subarcminute resolution imaging of radio sources at 74 MHz with the very large array, *Astron. J.*, **106**, 2218-2228, 1993.
- Kassim, N. E., and K. W. Weiler, (Eds.), *Low Frequency Astrophysics from Space*, Springer-Verlag, New York, 1990.
- Kellermann, K. I., et al., in *Working Papers, Astronomy and Astrophysics Panel Reports*, vol. 1, Nat. Acad., Washington, D. C., 1991.

- LaBelle, J., R. A. Treumann, M. H. Boehm, and K. Gewecke, Natural and man-made emissions at 1.0–5.6 MHz measured between 10 and 18 R_E , *Radio Sci.*, **24**, 725–737, 1989.
- Lee, L. C., and J. R. Jokipii, Strong scintillation in astrophysics, II, A theory of temporal broadening of pulses, *Astrophys. J.*, **201**, 532–543, 1975.
- McCoy, M., A predictive model of the HF noise environment at satellite heights, Ph.D. thesis, Iowa State Univ., Ames, 1995.
- McCoy, M., J. P. Basart, and M. Taylor, HF interference in space from terrestrial sources, in *Engineering, Construction, and Operations in Space: Proceedings of Fifth International Conference on Space '96*, edited by S. W. Johnson, pp. 854–860, Am. Soc. of Civ. Eng., New York, 1996.
- Ness, N. F., M. H. Acuna, R. P. Lepping, J. E. P. Connerney, K. W. Behannon, L. F. Burlaga, and F. M. Neubauer, Magnetic field studies by Voyager-1: Preliminary results at Saturn, *Science*, **212**, 211, 1981.
- Perley, R. A., Wide field imaging II: Imaging with non-coplanar arrays, in *Synthesis Imaging in Radio Astronomy*, edited by R. A. Perley, F. R. Schwab, and A. H. Bridle, pp. 259–275, Astron. Soc. of the Pac., San Francisco, Calif., 1989.
- Perley, R. A. and W. C. Erickson, A proposal for a large, low-frequency array located at the VLA site, *VLA Sci. Memo.*, **146**, Nat. Radio Astron. Obs., Socorro, N. M., 1994.
- Rees, N., The new Cambridge 38 MHz radio survey—1 steradian at 4 arcmin resolution and sub-Jansky sensitivity, in *Low Frequency Astrophysics from Space*, edited by N. E. Kassim and K. W. Weiler, pp. 204–213, Springer-Verlag, New York, 1990.
- Rees, N., A deep 38-MHz radio survey of the area $\delta > +60^\circ$ *Mon. Not. R. Astron. Soc.*, **244**, 233–246, 1990b.
- Rickett, B. J., Interstellar scattering and scintillation of radio waves, *Ann. Rev. Astron. Astrophys.*, edited by G. Burbidge, D. Layzer, and J. G. Phillips, **15**, 479–504, 1977.
- Roger, R. S., Low-frequency absorption due to IC 1805 and IC 1848, *Astrophys. J.*, **155**, 831–840, 1969.
- Sagitov, M. U., B. Bodri, V. S. Nazarenko, and K. G. Tadzhibidinov, *Lunar Gravimetry*, Academic, San Diego, Calif., 1986.
- Schwab, F. R., Relaxing the isoplanatism assumption in self-calibration; applications to low-frequency radio interferometry, *Astron. J.*, **89**, 1076–1081, 1980.
- Shain, C. A., M. M. Komesaraoff, and C. S. Higgins, A high resolution galactic survey at 19.7 Mc/s, *Aust. J. Phys.*, **14**, 508–514, 1961.
- Spangler, S. R., and J. W. Armstrong, Low-frequency angular broadening and diffuse interstellar plasma turbulence, in *Low Frequency Astrophysics from Space*, edited by N. E. Kassim and K. W. Weiler, pp. 155–164, Springer-Verlag, New York, 1990.
- Subrahmanya, C. R., Low frequency imaging and the non-isoplanatic atmosphere, in *Radio Interferometry: Theory, Techniques, and Applications*, edited by T. J. Cornwell and R. A. Perley, pp. 218–222, Astron. Soc. of the Pac., San Francisco, Calif., 1991.
- Thompson, A., J. Moran, G. and Swenson, *Interferometry and Synthesis in Radio Astronomy*, John Wiley, New York, 1986.
-
- J. P. Basart, Department of Electrical and Computer Engineering, Iowa State University, 333 Durham, Ames, IA 50011. (email: jpbasart@iastate.edu)
- J. O. Burns, Department of Astronomy, New Mexico State University, Las Cruces, NM 88003-0001. (email: jburns@nmsu.edu)
- S. P. Castillo, Department of Electrical Engineering, New Mexico State University, Las Cruces, NM 88003-0001. (email: scastill@emlab2.nmsu.edu)
- B. K. Dennison, Department of Physics, Virginia Polytechnic Institute, Blacksburg, VA 24061-0435. (email: dennison@astro.phys.vt.edu)
- N. E. Kassim and K. W. Weiler, Remote Sensing Division, Naval Research Laboratory, Washington, D. C. 20375-5351. (email: nkassim@shimmer.nrl.navy.mil; kweiler@sne.nrl.navy.mil)
- B. M. McCune, Physical Sciences Laboratory, New Mexico State University, Las Cruces, NM 8003-0001.

(Received August 22, 1995; revised July 30, 1996; accepted August 5, 1996.)